

The State Dependency of the Effective Pair Potential Parameters

by E. Keshavarzi^{1*}, F.S. Hashemi² and Z. Ghazvini³

¹Dept. of Chemistry, Isfahan University of Technology, Isfahan, 84154, Iran

²Dept. of Chemistry, Faculty of Sciences, Azzahra University, Tehran, Iran

³Dept. of Chemistry, Faculty of Basic Sciences, Mazandaran University, Babolsar, Iran

(Received November 12th, 2003; revised manuscript April 26th, 2004)

The state dependency of the effective pair potential parameters [$\epsilon_{eff}(T, \rho)$, $\sigma_{eff}(T)$] has been studied for gas, liquid and supercritical regions for different types of fluids. We have assumed that the configuration of potential energy between N molecules can be divided into independent pair clusters with an effective pair potential, in which the parameters of the potential are state dependent. We have obtained the values of $\epsilon_{eff}(T, \rho)$, and $\sigma_{eff}(T)$ using p - V - T data. The results show, that $\epsilon_{eff}(T, \rho)$ increases with density for those thermodynamic states, at which pair interactions are dominant, while it decreases with density for those systems, where triplet and higher clusters are dominant. Both $\epsilon_{eff}(T, \rho)$ and $\sigma_{eff}(T)$ decrease with temperature, which coincides with the literature data. A remarkable result of the present work is the determination of density, at which triplet clusters come into account. We have also shown new corresponding states for the effective well depth parameter, which is held for all examined fluids, including Ar, Xe, CH₄, N₂, CO, H₂O, CO₂, CH₃OH, C₂H₆ and C₆H₆ for different isotherms. A linear dependence of $\epsilon_{eff}(T, \rho)$ versus density and temperature on the zeno-line is predicted.

Key words: corresponding state, effective pair potential, equation of state, second virial coefficient, zeno-line

It is well known, that thermodynamic properties of fluids can be obtained from the knowledge of the interactions between molecules. Although there is no direct way to measure these interactions, it is common to get the intermolecular interactions, using the relation between thermodynamic properties and intermolecular interactions. This approach is known in literature as the inversion method [1], and some progress has been made in the past. Of course, most of the work on the inversion method has been done on the dilute gases, when only pair interactions are needed. Some of the properties, which have been used in the inversion method, are the shear viscosity [2], thermal conductivity [3], Joule-Thomson coefficients [4], volumetric virial coefficients [5] and, more recently, acoustic virial coefficients [6]. In dense systems, the total configuration of energy is not exactly equal to the sum of the pair energies [7]. Departures from additivity will cause the calculated potential parameters to vary with

* Author for correspondence (E-mail: keshavrz@cc.iut.ac.ir).

density and temperature. We named such state dependent pair potential as the “effective pair potential” (EPP).

The effective pair potential parameters, which have been obtained by various methods, show different state dependences [8–10]. These different results are related to the different definition of the EPP. For example the effect of the nonadditivity causes a decrease in $\varepsilon_{eff}(T, \rho)$ versus density [11], while ignoring the effect of second and third shell interactions for a central molecule causes an increase in $\varepsilon_{eff}(T, \rho)$ [8]. McLure *et al.* have presented a new theory to account the nonconformality of intermolecular potentials, which is used to obtain effective potentials [12]. The approximate nonconformal theory has been very successful for determining effective interaction parameters from $B_2(T)$ for variety of substances from noble gases to fluoro-n-alkanes [13]. Also this theory has been applied for the mixture of nonconformal potentials [14].

Our goal in this article is to investigate the state dependency of the EPP parameters for a wide range of densities and temperatures. In this work, the configuration of potential energy, U_N , is considered as the sum of independent pair clusters, that the intermolecular interactions in each cluster is EPP and we have obtained its state dependent parameters. This model has been used for gases, liquids and supercritical phases for all types of fluids including polar, non-polar and even hydrogen bonded systems for the states, in which the compressibility factor is less than unity (soft fluids).

RESULTS AND DISCUSSION

Effective second virial coefficient. The compressibility factor is related to the pair distribution function, $g(r)$, as:

$$Z = \frac{p}{\rho kT} = 1 - \frac{2\pi}{3} \frac{\rho}{kT} \int_0^\infty \frac{du(r)}{dr} g(r) r^3 dr \quad (1)$$

where $u(r)$ is the intermolecular pair potential. Z , p and ρ are compressibility factor, pressure and molar density, respectively and kT has its usual meaning. The assumptions in this equation are, that the configuration potential energy is pairwise additive and also the pair potential is central. It is possible to extract the exact second virial coefficient, B_2 , from the above integral and rewrite equation (1) as follows [11]:

$$\frac{p}{\rho kT} = 1 + B_2 \rho + \rho I \quad (2)$$

where:

$$B_2 = -\frac{2\pi}{3} \beta \int_0^\infty \frac{du(r)}{dr} e^{-\beta u(r)} r^3 dr = 2\pi \int_0^\infty (1 - e^{-\beta u(r)}) r^2 dr \quad (3)$$

$$I = \frac{2\pi}{3} \int_0^\infty f(r)[y(r) - 1] r^3 dr \quad (4)$$

$$y(r) = e^{\beta u(r)} g(r) \quad (5)$$

$$f(r) = -\beta \frac{du(r)}{dr} e^{-\beta u(r)} \quad (6)$$

where $\beta = 1/kT$. Ihm' Song and Mason [11] evaluated I by perturbation theory, and they found that I represents the repulsive part of the potential. At lower densities, the virial term of the integral, in (1), has an important role in the compressibility factor. At high densities the pressure of a liquid or highly compressed gas is usually large. Therefore, the main contribution to that integral comes from the repulsion. This is just a reflection of the fact, that the repulsive forces significantly contribute to the structure of a dense fluid. Below the critical temperature, the density for saturated vapor is so low that its behavior is largely described by B_2 . For a soft fluid (when $Z < 1$) the net effect of the forces in the compressibility factor is attraction, and the rearrangement of the (2) as $Z = 1 + (B_2 + I)\rho$, shows that the summation of B_2 and I should be negative. In other words, large negative values of B_2 over-come the contribution of the repulsion, which is represented by I . We define a new quantity, effective second virial coefficient, B_{2eff} , instead of the negative summation of B_2 and I . Since I is a density dependent parameter, B_{2eff} is also a density and temperature dependent parameter. Therefore, we have:

$$Z = 1 + B_{2eff}(T, \rho)\rho \quad (7)$$

The above equation may also be obtained by using the virial equation of state. The virial equation of state is

$$Z = 1 + B_2\rho + C\rho^2 + \dots \quad (8)$$

where C is the third virial coefficient. It is well known that B_2 is the contribution of the pair interaction in the compressibility factor, while C is a representation of the triplet interactions *etc.* For low densities, just the pair of intermolecular interactions is important, then $Z = 1 + B_2\rho$, but this approximation is not correct for higher densities. It is possible to consider Z as (7) and the effects of the other clusters, which are important at higher densities, included in B_{2eff} until this quantity remains negative. In this way we consider all the intermolecular interactions between N particles as an independent effective pair interaction.

At low densities these effective pair interactions should be equal to an isolated pair potential, but for higher densities they become density and temperature dependent. We considered the mathematical form of the effective pair potential the same as pair potential; just these parameters vary with thermodynamic states. We have used the Lennard-Jones potential with two state dependent parameters $[\varepsilon_{eff}(T, \rho), \sigma_{eff}(T)]$ as the effective pair potential. In this way the effective second virial coefficient is,

$$B_{2eff}(T, \rho) = -2\pi N \int_0^{\infty} (e^{-\beta u_{eff}(r)} - 1) r^2 dr \quad (9)$$

and the effective potential is,

$$u_{eff}(r, T, \rho) = 4\varepsilon_{eff}(T, \rho) \left[\left(\frac{\sigma_{eff}(T)}{r} \right)^{12} - \left(\frac{\sigma_{eff}(T)}{r} \right)^6 \right] \quad (10)$$

We will obtain the EPP parameters in the following section by finding B_{2eff} for any thermodynamic states.

Effective pair potential parameters. According to (10), there are two state dependent parameters, that should be obtained. It has been already determined by various inversion methods, that σ is a strongly temperature dependent parameter whereas its density dependence is negligible [15]. We have also supposed σ_{eff} to be just a temperature dependent parameter. The effective second virial coefficient is calculated from p - v - T data for any thermodynamic state, ((7)). Since the EPP is equal to the isolated pair potential at low densities, for any isotherms we have obtained σ_{eff} from B_{2eff} and ε_{iso} . $\varepsilon_{eff}(T, \rho)$ will be calculated from (9) for a range of density by using the effective second virial coefficient and knowing $\sigma_{eff}(T)$. We have done the above calculation for gases, liquids and supercritical fluids, when $B_{2eff}(T, \rho)$ is negative.

Gas phase. The values of $\sigma_{eff}(T)$ have been obtained from triple point to critical temperature by using the experimental values of B_{2eff} [16] and p - v - T data of Ar [17] as a simple atom. As it may be seen from Fig. 1, $\sigma_{eff}(T)$ decreases with increasing temperature. As temperature increases, the behavior of the system becomes similar to hard fluids and the repulsive branch of the effective pair potential becomes important. Similar behavior has been observed for other gases such as CO [18], N₂ [19], CH₄ [20], which is summarized in Fig. 1.

The effective potential well depth was obtained for Ar by using the values of $\sigma_{eff}(T)$ for some isotherms. According to Fig. 2(a), $\varepsilon_{eff}(T, \rho)$ increases with density for each isotherm, and decreases by temperature for a constant density. With increasing density for gas phase ($Z < 1$), pair clusters form and the attractive part of the pair potential becomes important. Therefore, if $\varepsilon_{eff}(T, \rho)$ is considered as a contribution of the attractive force, it should increase with density. But when the temperature increases, kinetic energy of the system increases and the behavior of the system changes to

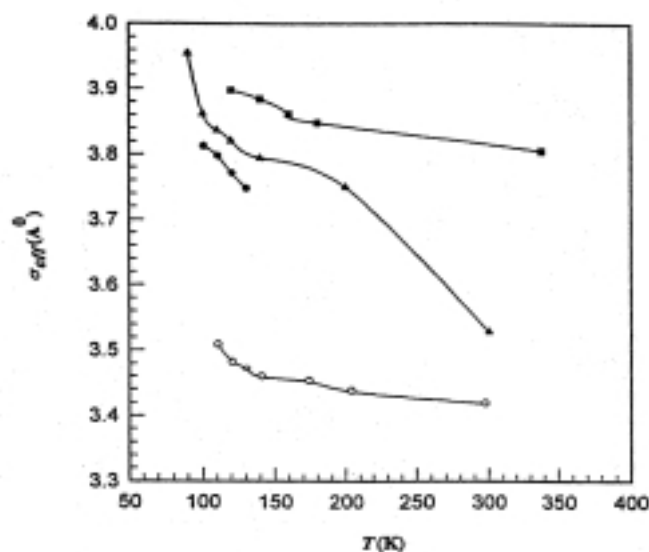


Figure 1. Temperature dependence of σ_{eff} for Ar (o), CO (●), N₂ (▲), CH₄ (■).

that of hard fluid. The repulsive branch of the effective pair potential has an important role, therefore $\epsilon_{eff}(T, \rho)$ decreases with temperature for a constant density. This behavior has been observed for all types of fluids including polar and non-polar, such as CO, N₂, CH₄, C₂H₆ [20], Xe [21], CO₂ [22] for different isotherms.

Liquid phase. $\epsilon_{eff}(T, \rho)$ has been obtained for a liquid phase, from triple point up to critical point by using the obtained values of $\sigma_{eff}(T)$ and B_{2eff} the same as in gas phase. Fig. 2(b) shows the behavior of $\epsilon_{eff}(T, \rho)$ versus density for 150 K, 140 K, 130 K, 120 K, 110 K, 100 K isotherms of Ar in liquid phase. At liquid density the effect of the third particle, which results likely from repulsive interactions, cannot be ignored, therefore the decrease of the ϵ_{eff} versus density is expected [1]. Also the average distance between particles in liquid is mostly around r_m (minimum of the pair potential) and the system becomes similar to hard fluids. Therefore, it can be shown that the effect of the existence of higher clusters causes $\epsilon_{eff}(T, \rho)$ decrease with density (Fig. 2(b)). Such a behavior is also shown for other liquids such as CO, N₂, C₂H₆, CH₄, Xe, CO₂, CH₃OH [23], and C₆H₆ [24] for different isotherms. Fig. 2(b) also shows that $\epsilon_{eff}(T, \rho)$ decreases with increasing temperature like for a gas phase.

Supercritical fluids. In the same way, we could determine $\epsilon_{eff}(T, \rho)$ for supercritical fluids, from critical temperature to Boyle temperature, for a full range of densities, at which $Z < 1$. Fig. 2 (c) shows this behavior for Ar, for two isotherms. For low densities, $\epsilon_{eff}(T, \rho)$ first increases with density and then decreases with it. It means that the behavior of $\epsilon_{eff}(T, \rho)$ is similar to a gas phase, until it reaches a maximum, then decreases with density such as for the liquid phase.

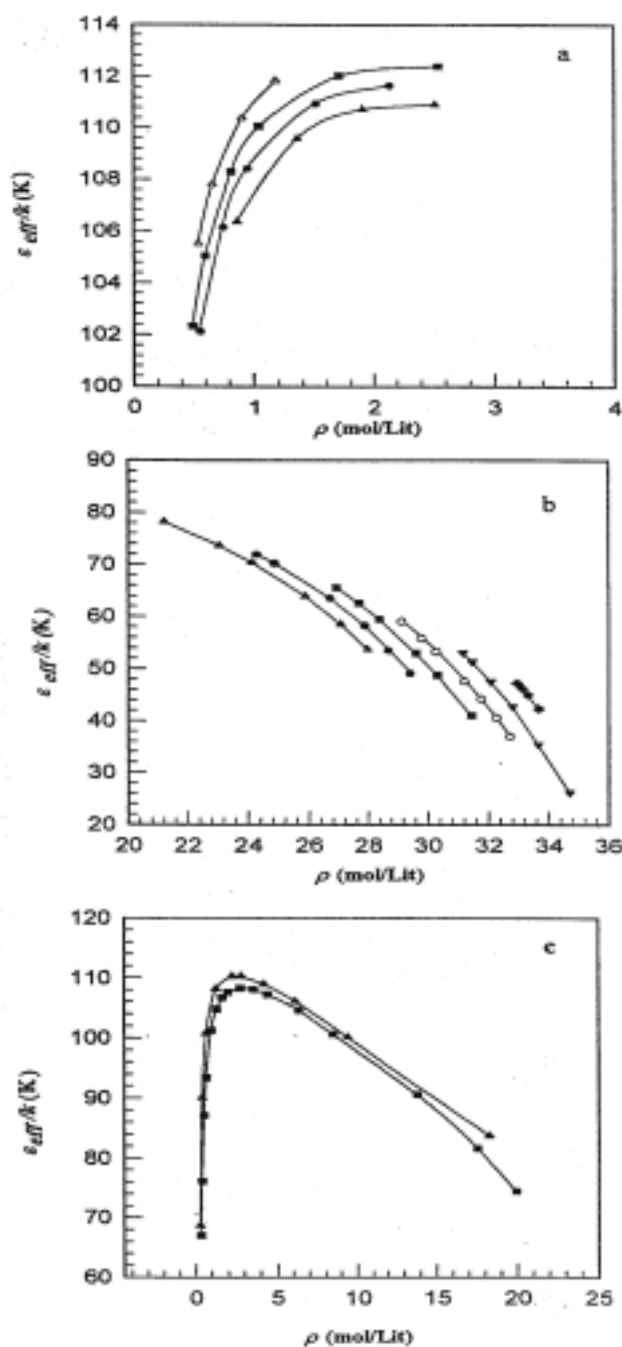


Figure 2. (a) The behavior of ϵ_{eff}/k versus density for different isotherms of Ar for gas phase (▲) 150 K, (●) 140 K, (■) 130 K, (Δ) 120 K. (b) The behavior of ϵ_{eff}/k versus density for liquid phase of Ar for (▲) 150 K, (●) 140 K, (■) 130 K, (○) 120 K, (▼) 110 K, (◆) 100 K isotherms. (c) The variation of ϵ_{eff}/k for Ar in the supercritical region versus density for (▲) 160 K and (■) 200 K isotherms.

The interesting point, which was obtained, is the different behavior of $\varepsilon_{eff}(T, \rho)$ versus density for low and high-density regions. In fact, the decrease of $\varepsilon_{eff}(T, \rho)$ with density is the representation of the existence of the triplet or higher interaction between molecules. On the other hand, we have shown that the compressibility factor calculated by using virial equation of state by considering the two terms, $Z = 1 + B_2\rho$, is equal to the experimental compressibility factor, Z_{exp} , up to the density at which $\varepsilon_{eff}(T, \rho)$ has its maximum value (Fig. 3). Because in the truncated virial equation of state after two terms, just the pair interaction is considered. When it can present the experimental compressibility factor, it can be concluded, that just pair clusters exist in the system. In this way we have shown that there is a specific density for each isotherms, at which the interactions may change from two bodies to many body. Such a behavior has been also observed for all types of fluids for different isotherms. The results are summarized in Table 1 for Ar, CO, CO₂, C₂H₆ and N₂ for several isotherms.

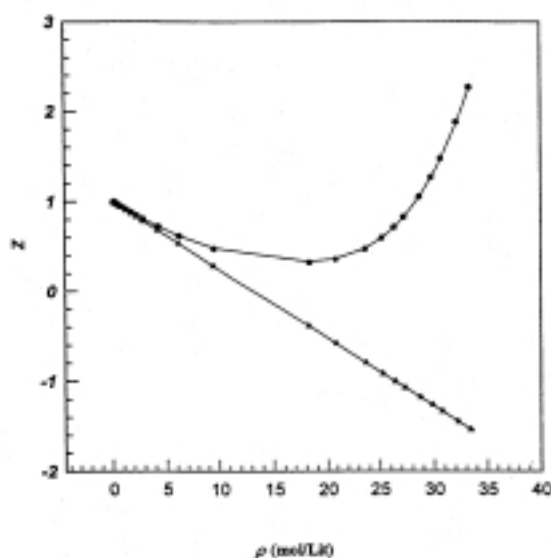


Figure 3. Comparison of $Z = 1 + B_{2exp} \rho$ (\blacktriangle) with the experimental compressibility factor (\bullet) for 160 K isotherm of Ar.

Corresponding states for the behavior of $B_{2eff}(T, \rho)$ versus $\varepsilon_{eff}(T, \rho)$. We have observed that the obtained values of $\varepsilon_{eff}(T, \rho)$ exhibit a linear behavior versus $B_{2eff}(T, \rho)$ for gas and liquid phase. Figs. 4(a,b) show such a behavior for Ar. If we divide the integral of the effective second virial coefficient into two parts, $(0-\sigma)$ and $(\sigma-\infty)$, we obtain:

$$B_{2eff}(T, \rho) = -2\pi N \left[\int_0^{\sigma} (e^{-\beta u_{eff}} - 1) r^2 dr + \int_{\sigma}^{\infty} (e^{-\beta u_{eff}} - 1) r^2 dr \right] \quad (11)$$

We have supposed that u_{eff} is approximately equal to infinity for the first integral (it is correct just for hard fluids) and used the Taylor expansion for the exponential part in the second integral:

$$B_{2eff}(T, \rho) = \frac{2}{3} \pi N \sigma_{eff}^3(T) - \frac{16\pi N}{9} \sigma_{eff}^3(T) \frac{\varepsilon_{eff}(T, \rho)}{kT} + \dots \quad (12)$$

(12) shows a linear relation between $B_{2eff}(T, \rho)$ and $\varepsilon_{eff}(T, \rho)$, if just the first term of Taylor expansion has been considered for any isotherm.

Table 1. The specific density at which $\varepsilon_{eff}(T, \rho)$ has its maximum value for different isotherms for several compounds.

Compound	T (K)	ρ (mol/Lit)	ε/k (K)
Ar	160	2.4820	110.4065
Ar	200	2.6842	108.2003
CO	140	0.4477	98.1394
CO	150	0.4145	96.1319
CO ₂	450	3.2503	173.2253
N ₂	130	4.5674	85.0128
C ₂ H ₆	400	4.0439	177.0934

(12) was examined by using the calculated $B_{2eff}(T, \rho)$ and $\varepsilon_{eff}(T, \rho)$ for each isotherm of Ar. The results show an excellent agreement for Ar in the gas phase for 150 K, 140 K, 130 K, and 120 K isotherms (Fig. 4(a)) and for liquid Ar at 150 K, 140 K, 130 K, 120 K, 110 K, 100 K isotherms (Fig. 4(b)). (12) may be rearranged as:

$$\frac{B_{2eff}(T, \rho)}{\sigma_{eff}^3(T)} = \frac{2}{3} \pi N - \frac{16\pi N}{9T} \frac{\varepsilon_{eff}(T, \rho)}{k} + \dots \quad (13)$$

which show that if $B_{2eff}(T, \rho)/\sigma_{eff}^3(T)$ is plotted *versus* $\varepsilon_{eff}(T, \rho)/kT$, it should yield a unique and the same line for all kinds of fluids at any temperature. We examined such corresponding states for all kinds of fluids (including Ar, CO, N₂, CH₄, Xe, C₆H₆, CO₂, and CH₃OH) at any temperature in the gas phase in Fig. 5(a) and for liquid region in Fig. 5(b). According to Fig. 5, this corresponding state is held for all types of fluids at any temperature. The results are very remarkable, because they include the system with hydrogen bonding, such as CH₃OH. If the higher terms of the (12) are also considered, $B_{2eff}(T, \rho)$ will be at least a quadratic function *versus* $\varepsilon_{eff}(T, \rho)/k$, that is observed for the supercritical phase because of wide density range in this region. Fig. 4(c) shows such a behavior for 200 K, 160 K isotherms of Ar.

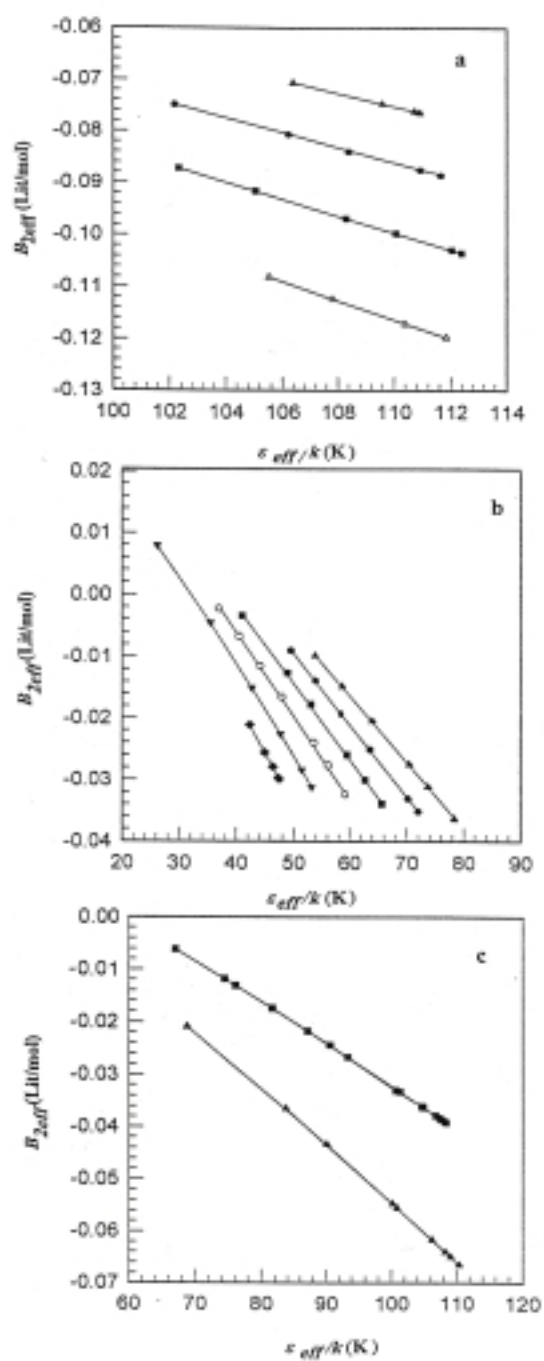


Figure 4. (a) The linear behavior of $B_{2,eff}$ versus ϵ_{eff}/k for Ar in the gas phase for different isotherms, (\blacktriangle) 150 K, (\bullet) 140 K, (\blacksquare) 130 K, (\triangle) 120 K. (b) Same as Figure 4(a) for Ar in the liquid phase, 150 K (\blacktriangle), 140 K (\bullet), 130 K (\blacksquare), 120 K (\circ), 110 K (\blacktriangledown), 100 K (\blacklozenge). (c) Same as Figure 4(a) for Ar in the supercritical phase for different isotherms, 160 K (\blacktriangle), 200 K (\blacksquare).

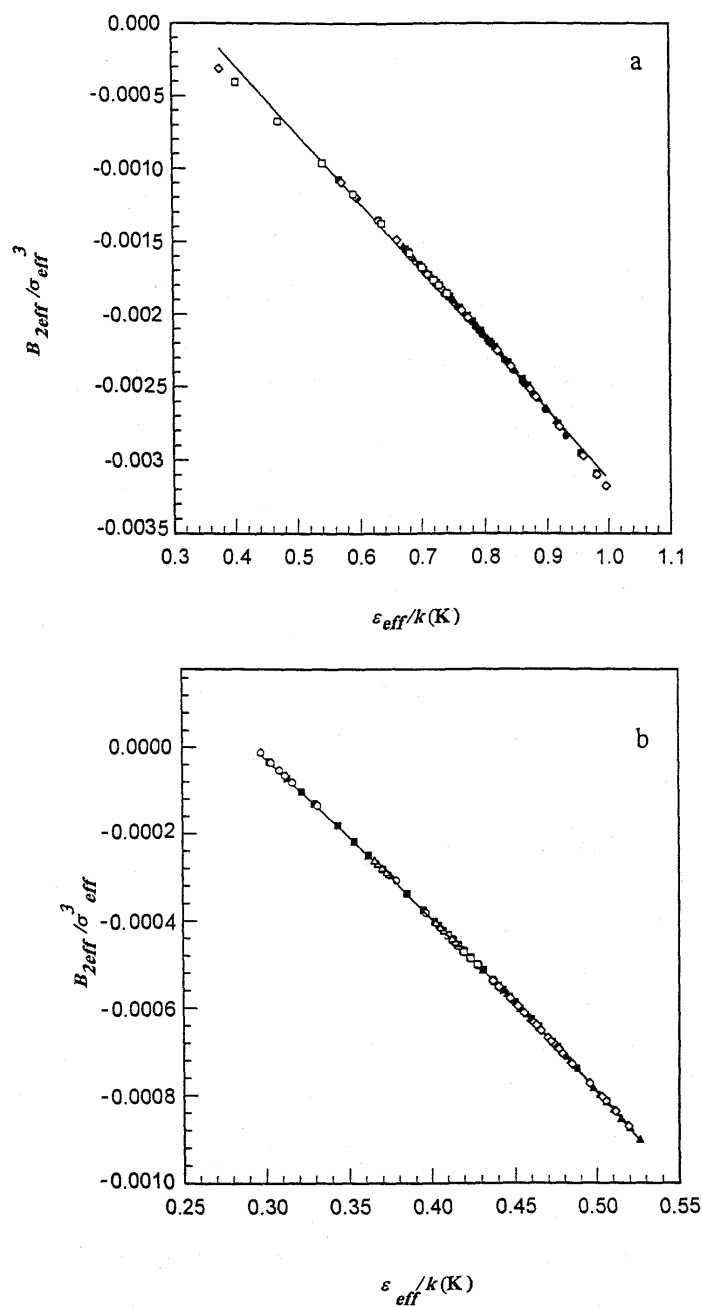


Figure 5. ((a) The corresponding states of B_{2eff}/σ_{eff}^3 and ϵ_{eff}/kT for all isotherms of all kinds of fluid including, Ar (●), CO (▲), N₂ (■), CH₄ (◇), Xe (○), C₆H₆ (◆), CO₂ (□), CH₃OH (Δ) in the gas phase. (b) Same as Figure 5(a) for liquid phase, Ar (●), CO (▲), N₂ (■), CH₄ (◇), Xe (○), C₆H₆ (◆), CO₂ (□), CH₃OH (Δ).

Zeno-line. A linear relation exists for temperature *versus* density for thermodynamic states at which Z equals to unity, this line is named zeno-line [25] (Fig. 6(a)). The intercept of the zeno-line is specified by Boyle temperature (T_B). It is remarkable that the linearity of zeno-line remains even in the dense fluid region, as it gets near the triple point. Although the intermolecular interactions are very important in dense systems, this linear behavior shows that the attractive and repulsive contributions are in a dynamic balance along the zeno-line [26]. According to this linearity we have

$$T = \alpha - \beta\rho \quad (14)$$

where α and β are constants dependent on the types of fluids, when $\rho \rightarrow 0$, then $\alpha = T_B$. The linear behavior for $\epsilon_{eff}(T, \rho)/k$ *versus* density and also temperature was observed on the zeno-line. Fig. 6(b) and Fig. 7 show these behaviors for Ar.

The other examined fluids also show such a behavior (Table 1). We have also shown the behavior of $\epsilon_{eff}(T, \rho)/k$ *versus* density and temperature for $Z = 0.8$ for Ar in Figs. 6(a,b), (it shows a curvature). Fig. 6(b) shows that at low densities the value of $\epsilon_{eff}(T, \rho)/k$ is nearly equal to ϵ_{iso} and decreases with increasing density. The effect of the existence of higher clusters at high densities causes a decrease in $\epsilon_{eff}(T, \rho)/k$. Since $B_{2eff}(T, \rho)$ is equal to zero on zeno-line, (12) may be rearranged as:

$$\epsilon_{eff}(T, \rho)/k = 0.37T \quad (15)$$

which shows that the slope of $\epsilon_{eff}(T, \rho)/k$ *versus* temperature on the zeno-line should be equal to 0.37, if two approximations which are used to derive (15) cancel each other completely. We examined that case for different fluids such as Ar, N₂, CH₄, Xe, and CO₂. The slopes are summarized in Table 2, which do not show the exact agreement with (15), but the linear behavior with the same slope has been observed.

Conclusions. The state dependency of the effective pair potential parameters has been obtained in this work [27]. We have shown the variation of $\epsilon_{eff}(T, \rho)/k$ with density in a wide range of thermodynamic states.

In the gas phase just two body intermolecular interactions are important and by increasing density, their contributions become more important. Therefore, $\epsilon_{eff}(T, \rho)/k$ increases with density, and it decreases at high densities. In a real system, when contributions of triplet and higher-order interactions become very important, the variation of $\epsilon_{eff}(T, \rho)/k$ *versus* density is different. The effective pair potential parameters, $\epsilon_{eff}(T, \rho)$ and $\sigma_{eff}(T)$, decrease with temperature. The existence of a new corresponding state between $\epsilon_{eff}(T, \rho)/k$, and $B_{2eff}(T, \rho)$ shows a universal linear dependence for intermolecular interactions of different types of molecules. This linear dependence for all type of fluids, including nonpolar, polar and hydrogen-bonded systems for all isotherms is very remarkable. The final interesting point is the linear behavior of $\epsilon_{eff}(T, \rho)/k$ *versus* density and also temperature on the zeno-line. In this way, we are able to divide fluids into soft and hard by this linear behavior.

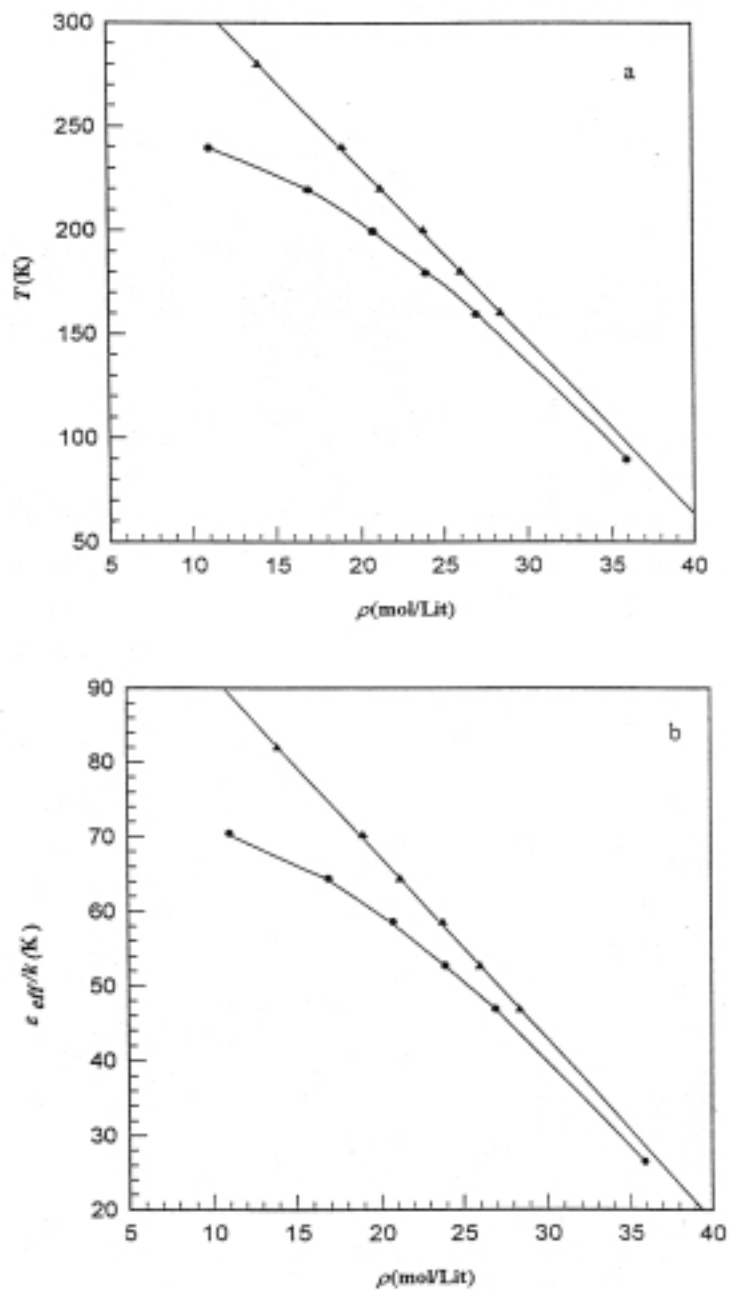


Figure 6. (a) The linear behavior of density *versus* temperature for zeno-line (▲), compared with $Z=0.8$ (●) of Ar. (b) The linear behavior of ϵ_{eff}/k *versus* density for Ar on zeno-line (▲), compared with $Z=0.8$ (●).

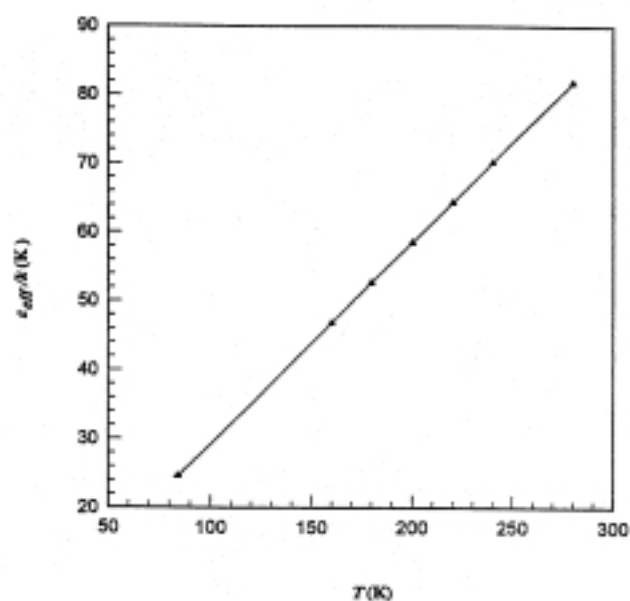


Figure 7. The linear behavior of ϵ_{eff}/k versus temperature for $Z = 1$ (▲).

Table 2. The slope and intercept of $\epsilon_{eff}(T, \rho)$ versus temperature on zeno-line for different kinds of fluids.

Compound	T range (K)	ρ range (mol/Lit)	intercept T_B (K)	slope
Ar	331–497	0.8–12.5	520.1	0.29
N ₂	231–319	0.9–11.9	326.2	0.29
CH ₄	331–497	8.0–12.5	509.3	0.29
Xe	273–423	13.8–19.4	793.4	0.29
CO ₂	273–653	4.0–25.4	721.7	0.29

Acknowledgment

We would like to acknowledge the Isfahan University of Technology Researches for their financial support. Heartfelt thanks go to Mrs. Khaleghi and Dr. Fotouhi for their helps.

REFERENCES

1. Maitland G.C., Rigby M., Smith E.B. and Wakeham W.A., *Intermolecular Forces. Their Origin and Determination*, Clarendon Press, Oxford, 1981.
2. Clarke A.G. and Smith E.B., *J. Chem. Phys.*, **48**, 3988 (1968); Dawe R.A. and Smith E.B., *J. Chem. Phys.*, **52**, 693 (1970).
3. Gubbins K.E., *J. Chem. Phys.*, **48**, 1404 (1968).
4. Keshavarzi E., Parsafar G. and Najafi B., *Int. J. Thermophys.*, **20**, 643 (1999).
5. Maitland G.C. and Wakeham W.A., *Mol. Phys.*, **35**, 1443 (1978).
6. Trusler J.P.M., *Physical Acoustics and Metrology of Fluids*, Adam Hilger, Bristol, 1991.
7. Ramos J.E., Del Rio F. and Estranda-Alexanders F., *Int. J. Thermophys.*, **20**, 631 (1999).
8. Parsafar G., Kermanpour F. and Najafi B., *J. Phys. Chem. B*, **103**, 7287 (1999).
9. Attard P. and Parker J.L., *Phys. Rev. A*, **46**, 7959 (1992).
10. Del Rio F., Ramos J.E., Gil-Villegas A. and McLure I.A., *J. Phys. Chem.*, **100**, 9104 (1996).
11. Song Y. and Mason E.A., *J. Chem. Phys.*, **91**, 7840 (1989).
12. McLure I.A., Ramos J.E. and Del Rio F., *J. Phys. Chem. B*, **103**, 7019 (1999).
13. Ramos J.E., Del Rio F. and McLure I.A., *Phys. Chem. Chem. Phys.*, **3**, 2634 (2001).
14. Del Rio F., Ramos J.E. and McLure I.A., *Phys. Chem. Chem. Phys.*, **1**, 4937 (1999).
15. Reed T.M. and Gubbins K.E., *Applied Statistical Mechanics*, Chemical Engineering Series of Fluids, McGraw-Hill, NY, 1973.
16. Dymond J.H. and Smith E.B., *The Virial Coefficients of Pure Gases and Mixtures. A Critical Compilation*, Oxford University, NY, 1980.
17. Stewart R.B. and Jacobsen R.T., *J. Phys. Chem. Ref. Data*, **18**, 639 (1989).
18. Goodwin R.D., *J. Phys. Chem. Ref. Data*, **14**, 849 (1985).
19. Jacobsen R.T., Stewart R.B. and Jahangiri M., *J. Phys. Chem. Ref. Data*, **15**, 735 (1986).
20. Younglove B.A. and Ely J.F., *J. Phys. Chem. Ref. Data*, **16**, 577 (1987).
21. Sifner O. and Klomfar J., *J. Phys. Chem. Ref. Data*, **23**, 63 (1994).
22. Span R. and Wagner W., *J. Phys. Chem. Ref. Data*, **25**, 1509 (1996).
23. Goodwin R.D., *J. Phys. Chem. Ref. Data*, **16**, 799 (1987).
24. Goodwin R.D., *J. Phys. Chem. Ref. Data*, **17**, 1541 (1988).
25. Kutney M.C., Reagan M.T., Smith K.A., Tester J.W. and Herschbach D.R., *J. Phys. Chem. B*, **104**, 9513 (2000).
26. Brandl H., *Z. Phys. Chem.*, **260**, 174 (1979).
27. Keshavarzi E. *et al.* presented in 17th IUPAC Conference on Chemical Thermodynamics, 2002, p. 25.